PHYSICAL REVIEW C **78**, 054902 (2008)

Landau hydrodynamics reexamined

Cheuk-Yin Wong*
Physics Division, Oak Ridge National Laboratory, Oak Ridge, Tennessee 37831, USA
(Received 8 August 2008; published 6 November 2008)

We review the formulation of Landau hydrodynamics and find that the rapidity distribution of produced particles in the center-of-mass system should be more appropriately modified as $dN/dy \propto \exp\{\sqrt{y_b^2 - y^2}\}$, where $y_b = \ln\{\sqrt{s_{NN}}/m_p\}$ is the beam nucleon rapidity, instead of Landau's original distribution, $dN/dy(\text{Landau}) \propto \exp\{\sqrt{L^2 - y^2}\}$, where $L = \ln\{\sqrt{s_{NN}}/2m_p\}$. The modified distribution agrees better with experimental dN/dy data than the original Landau distribution and can be represented well by the Gaussian distribution, $dN/dy(\text{Gaussian}) \propto \exp\{-y^2/2L\}$. Past successes of the Gaussian distribution in explaining experimental rapidity data can be understood, not because it is an approximation of the original Landau distribution, but because it is in fact a close representation of the modified distribution. Predictions for pp and AA collisions at LHC energies in Landau hydrodynamics are presented.

DOI: 10.1103/PhysRevC.78.054902 PACS number(s): 25.75.Ag

I. INTRODUCTION

Recent experimental data in high-energy heavy-ion collisions [1–3] reveal that the rapidity distributions of produced particles do not exhibit the plateau structure of Hwa-Bjorken hydrodynamics [4,5]. On the contrary, the Landau hydrodynamical model [6,7] yields results that agree with experiment [1–3]. Landau hydrodynamics provides a plausible description for the evolution of the dense hot matter produced in high-energy heavy-ion collisions. Its dynamics during the first stage of the one-dimensional longitudinal expansion can be solved exactly and the one-dimensional longitudinal expansion problem admits simple approximate solutions [6–21]. The subsequent three-dimensional motion can be solved approximately to give rise to predictions that come close to experimental data [1–3,6,7]. A critical re-examination of Landau hydrodynamics will make it a useful tool for the description of the evolution of the produced dense matter.

Quantitative analyses of Landau hydrodynamics in Refs. [1–3,11] use a Gaussian form of the Landau rapidity distribution [6,7]

$$dN/dy(\text{Gaussian}) \propto \exp\{-y^2/2L\}, \tag{1.1}$$

where L is the logarithm of the Lorentz contraction factor $\gamma = \sqrt{s_{NN}}/2m_p$,

$$L = \ln\gamma = \ln(\sqrt{s_{NN}}/2m_p), \tag{1.2}$$

$\sqrt{s_{NN}}/2$ is the center-of-mass energy per nucleon, and m_p is the proton mass. This Gaussian rapidity distribution gives theoretical rapidity widths that agree with experimental widths for many different particles in central AuAu collisions, to within 5 to 10%, from BNL Alternating Gradient Synchrotron (AGS) energies to BNL Relativistic Heavy-Ion Collider (RHIC) energies [1–3]. The Landau hydrodynamical model also gives the correct energy dependence of the observed total charged multiplicity and the limiting fragmentation property at forward rapidities [2,3]. A similar analysis in terms of the pseudorapidity variable η at zero pseudorapidity has been carried out in Ref. [22].

The successes of these analyses indicate that Landau hydrodynamics can be a reasonable description. However, they also raise many unanswered questions. First, the original Landau result stipulates the rapidity distribution to be [6,7]

$$dN/d\lambda(\text{Landau}) \propto \exp\{\sqrt{L^2 - \lambda^2}\}, \tag{1.3}$$

where the symbol λ is often taken to be the rapidity variable y in Refs. [1–3,11]. In the original work of Landau and his collaborator in Refs. [6,7], the variable λ is used to represent the polar angle θ as $e^{-\lambda} = \theta$; there is the question whether the variable λ in the Landau rapidity distribution (1.3) should be taken as the rapidity variable y [1–3,11] or the pseudorapdity variable η [22] appropriate to describe the polar angle. Such a distinction between the rapidity and pseudorapidity variables is quantitatively important because the shape of the distributions in these two variables are different near the region of small rapidities [23]. Second, the Gaussian rapidity distribution (1.1) used in the analyses of Refs. [1–3] is only an approximate representation of the original Landau distribution (1.3) in the region of $|\lambda| \ll L$, but differs from the original Landau distribution (1.3) in other rapidity regions. They are in fact different distributions. While the original Landau distribution can be considered to receive theoretical support in Landau hydrodynamics as justified in Refs. [6,7], a firm theoretical foundation for the Gaussian distribution (1.1) in Landau hydrodynamics is still lacking. Finally, if one does not use the approximate representation of the Gaussian distribution (1.1) but keeps the original Landau distribution (1.3), then there is the quantitative question [14] whether this original Landau distribution will give results that agree with experimental data.

In view of the above unanswered questions, our task in reviewing the Landau hydrodynamical model will need to ensure that we are dealing with the rapidity variable y and not the pseudorapidity variable η. We need to be careful about various numerical factors so as to obtain a quantitative determination of the parameters in the final theoretical results. Finally, we need to ascertain whether the theoretical results

*wongc@ornl.gov

agree with experimental data. If we succeed in resolving the unanswered questions, we will pave the way for the application of Landau hydrodynamics to other problems in high-energy heavy-ion collisions.

II. TOTAL NUMBER OF PRODUCED CHARGED PARTICLES

Landau hydrodynamics involves two different aspects: the global particle multiplicity and the differential rapidity distribution. Landau assumed that the hydrodynamical motion of the fluid after the initial collision process is adiabatic. He argued that the only thing that can destroy adiabaticity would be the shock waves that, however, occur at the initial compressional stage of the collision process [24]. Landau therefore assumed that during the longitudinal and transverse expansion phase under consideration, the entropy content of the individual region remains unchanged. The total entropy of the system is therefore unchanged and can be evaluated at the initial stage of the overlapped and compressed system.

From the consideration of the thermodynamical properties of many elementary systems, Landau found that the ratio of the entropy density to the number density for a thermally equilibrated system is nearly a constant within the temperature regions of interest. Landau therefore postulated that the number density is proportional to the entropy density. Thus, by collecting all fluid elements, the total number of particles is proportional to the total entropy. As the total entropy of the system is unchanged during the hydrodynamical evolution, the total number of observed particles can be determined from the initial entropy of the system.

We work in the center-of-mass system and consider the central collision of two equal nuclei, each of mass number A, at a nucleon-nucleon center-of-mass energy $\sqrt{s_{NN}}$. Consider first the case of central AA collisions with $A \gg 1$ such that nucleons of one nucleus collide with a large numbers of nucleons of the other nucleus and the whole energy content is used in particle production. The total energy content of the system is

$$E = \sqrt{s_{NN}} A. \tag{2.1}$$

The initial compressed system is contained in a volume that is Lorentz contracted to become

$$V = \frac{4\pi}{3}(r_0 A^{1/3})^3/\gamma, \tag{2.2}$$

where $r_0 = 1.2$ fm. The energy density of the system is therefore

$$\epsilon = E/V = \gamma\sqrt{s_{NN}}/(4\pi r_0^3/3). \tag{2.3}$$

For a system in local thermal equilibrium, the entropy density σ is related to the energy density by

$$\sigma = \text{constant}\,\epsilon^{3/4}. \tag{2.4}$$

The total entropy content of the system is therefore

$$S = \sigma V = \text{constant}\, s_{NN}^{1/4} A. \tag{2.5}$$

With Landau's assumption relating entropy and particle number, $N \propto S$, the total number of particles produced is

$$N \propto s_{NN}^{1/4} A, \tag{2.6}$$

and the total number of produced charged particles per participant pair is

$$N_{\text{ch}}/A = N_{\text{ch}}/(N_{\text{part}}/2) = K(\sqrt{s_{NN}}/\text{GeV})^{1/2}, \tag{2.7}$$

where K can be determined phenomenologically by comparison with experimental data.

In Fig. 1(a), we show the PHOBOS data of $N_{\text{ch}}/(N_{\text{part}}/2)$ as a function of $(\sqrt{s_{NN}}/\text{GeV})^{1/2}$ for central AuAu collisions in RHIC [2,3]. The RHIC AuAu data can be parametrized as

$$N_{\text{ch}}/(N_{\text{part}}/2) = 1.135 + 2.019(\sqrt{s_{NN}}/\text{GeV})^{1/2}, \tag{2.8}$$

where the constant 1.135 arises from the leading baryons. The constant K as determined from the data is $K = 2.019$, which agrees with the earlier estimate of $K = 2$ [6,7].

Consider next pp and $p\bar{p}$ collisions in which not all the energy of $\sqrt{s_{NN}}$ is used in particle production, as the leading particles carry a substantial fraction of the initial energy. If we denote the particle production energy fraction in pp and $p\bar{p}$ collisions by ξ, then Eq. (2.7) is modified to be

$$N_{\text{ch}} = K(\xi\sqrt{s_{NN}}/\text{GeV})^{1/2}. \tag{2.9}$$

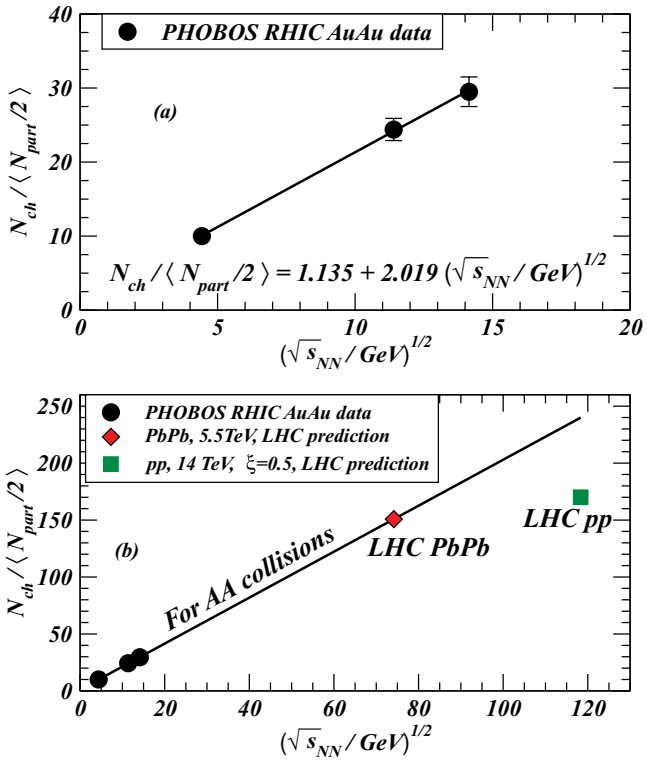

FIG. 1. (Color online) Total number of produced charged particles per pair of participants, $N_{\text{ch}}/(N_{\text{part}}/2)$, as a function of $(\sqrt{s_{NN}}/\text{GeV})^{1/2}$. (a) PHOBOS $N_{\text{ch}}/(N_{\text{part}}/2)$ data for central AuAu collisions at different $(\sqrt{s_{NN}}/\text{GeV})^{1/2}$ and the Landau hydrodynamical model fit, and (b) the extrapolation of the charged multiplicity in Landau hydrodynamical model to pp and PbPb collisions at LHC energies.

Comparison of the charged particle multiplicity in pp and $p\bar{p}$ collisions indicates that the particle production energy fraction ξ for pp and $p\bar{p}$ collisions is approximately 0.5 [2,3,23,25]. In contrast, the case of RHIC AA data in high-energy heavy-ion collisions corresponds to full nuclear stopping with $\xi = 1$ [2,3].

In Fig. 1(b), we show the predictions for the charge particle multiplicity per pair of participants for collisions at CERN Large Hadron Collider (LHC) energies. For pp collisions at 14 TeV with a particle production energy fraction $\xi = 0.5$, $N_{\rm ch}$ is predicted to be 170. For central PbPb collisions at $\sqrt{s_{NN}} = 5.5$ TeV with full nuclear stopping ($\xi = 1$), $N_{\rm ch}/(N_{\rm part}/2)$ is predicted to be 151.

III. LONGITUDINAL HYDRODYNAMICAL EXPANSION

We proceed to examine the dynamics of the longitudinal and transverse expansions in the collision of two equal nuclei of diameter a. The disk of initial configuration in the center-of-mass system has a longitudinal thickness Δ given by

$$\Delta = a/\gamma, \tag{3.1}$$

as depicted in Fig. 2 with major diameters a_x and a_y and the reaction plane lying on the x-z plane. Depending on the impact parameter, the dimensions of the disk obey $a_x \leqslant a_y \leqslant a$. For a central collision, $a_x = a_y = a$.

Among the coordinates $(t, z, x, y) \equiv (x^0, x^1, x^2, x^3)$ used to describe the fluid, Landau suggested a method to split the problem into two stages. The first stage consists of independent expansions along the longitudinal and the transverse directions. For the longitudinal expansion, the equation of hydrodynamics is

$$\frac{\partial T^{00}}{\partial t} + \frac{\partial T^{01}}{\partial z} = 0, \tag{3.2}$$

$$\frac{\partial T^{01}}{\partial t} + \frac{\partial T^{11}}{\partial z} = 0, \tag{3.3}$$

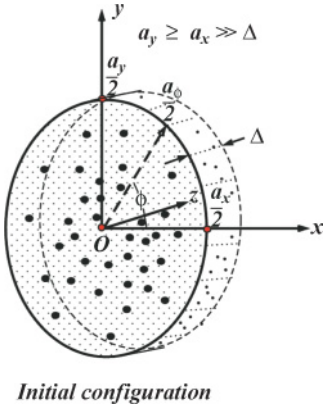

FIG. 2. (Color online) Initial configuration in the collision of two heavy equal nuclei in the center-of-mass system. The region of nuclear overlap consists of a thin disk of thickness Δ along the longitudinal z axis. The reaction plane is designated to lie on the x-z plane, and the transverse radii are $a_x/2$ and $a_y/2$.

where

$$T^{\mu\nu} = (\epsilon + p)u^\mu u^\nu - p g^{\mu\nu}. \tag{3.4}$$

We shall assume for simplicity the relativistic equation of state

$$p = \epsilon/3. \tag{3.5}$$

To ensure that we deal with rapidities, we represent the velocity fields (u^0, u^1) by the flow rapidity y,

$$u^0 = \cosh y, \tag{3.6a}$$

$$u^1 = \sinh y. \tag{3.6b}$$

We introduce the light-cone coordinates t_+ and t_-,

$$t_+ = t + z, \tag{3.7a}$$

$$t_- = t - z, \tag{3.7b}$$

with their logarithmic representations (y_+, y_-) defined by

$$y_\pm = \ln\{t_\pm/\Delta\} = \ln\{(t \pm z)/\Delta\}. \tag{3.8}$$

The hydrodynamical Eqs. (3.2) and (3.3) become

$$\frac{\partial \epsilon}{\partial t_+} + 2\frac{\partial(\epsilon e^{-2y})}{\partial t_-} = 0, \tag{3.9a}$$

$$2\frac{\partial(\epsilon e^{2y})}{\partial t_+} + \frac{\partial \epsilon}{\partial t_-} = 0. \tag{3.9b}$$

For the first stage of one-dimensional hydrodynamics, the exact solution for an initially uniform slab has been obtained and discussed in Refs. [7–21]. There are, in addition, simple approximate solutions [6,7]. In view of the matching of the solution to an approximate three-dimensional motion in the second stage, it suffices to consider the approximate solutions given by [7]

$$\epsilon(y_+, y_-) = \epsilon_0 \exp\left\{-\frac{4}{3}(y_+ + y_- - \sqrt{y_+ y_-})\right\}, \tag{3.10a}$$

$$y(y_+, y_-) = (y_+ - y_-)/2. \tag{3.10b}$$

The flow rapidity equation of Eq. (3.10b) can also be written alternatively as

$$e^{2y(y_+, y_-)} = \frac{t_+}{t_-} = \frac{t+z}{t-z}. \tag{3.11}$$

The constant ϵ_0 in Eq. (3.10a) is related to the initial energy density at (y_{+0}, y_{-0}) by

$$\epsilon_0 = \epsilon(y_{+0}, y_{-0})e^{\phi_0}, \tag{3.12}$$

where ϕ_0 is

$$\phi_0 = \frac{4}{3}(y_{+0} + y_{-0} - \sqrt{y_{+0} y_{-0}}). \tag{3.13}$$

We can easily prove by direct substitution that Eqs. (3.10a) and (3.10b) [or Eq. (3.11)] are approximate solutions of the hydrodynamical Eqs. (3.9a) and (3.9b). First, substituting Eq. (3.11) into the hydrodynamical equations, we obtain

$$\frac{\partial \epsilon}{\partial t_+} + 2\left[\frac{\partial \epsilon}{\partial t_-} + \frac{\epsilon}{t_-}\right]\frac{t_-}{t_+} = 0, \tag{3.14a}$$

$$2\left[\frac{\partial \epsilon}{\partial t_+} + \frac{\epsilon}{t_+}\right]\frac{t_+}{t_-} + \frac{\partial \epsilon}{\partial t_-} = 0. \tag{3.14b}$$

We write out t_-/t_+ in the second equation and substitute it into the first equation, and we get

$$\frac{\partial\epsilon}{\partial t_+}\frac{\partial\epsilon}{\partial t_-} - 4\left[\frac{\partial\epsilon}{\partial t_-} + \frac{\epsilon}{t_-}\right]\left[\frac{\partial\epsilon}{\partial t_+} + \frac{\epsilon}{t_+}\right] = 0. \quad (3.15)$$

We multiply this expression by t_+t_- and change into the logarithm variables y_+ and y_-, then the above equation becomes

$$\frac{\partial\epsilon}{\partial y_+}\frac{\partial\epsilon}{\partial y_-} - 4\left[\frac{\partial\epsilon}{\partial y_-} + \epsilon\right]\left[\frac{\partial\epsilon}{\partial y_+} + \epsilon\right] = 0. \quad (3.16)$$

If we now substitute Eq. (3.10a) for ϵ into the left-hand side of the above equation, we find that the left-hand side gives zero, indicating that Eqs. (3.10a) and (3.10b) are indeed approximate solutions of the hydrodynamical equation.

The simple approximate solutions of Eqs. (3.10a) and (3.10b) have limitations. They cannot describe the boundary layers for which $|t \pm z| < \Delta$ and $y_\pm$ becomes negative. In highly relativistic collisions, the tail regions excluded from the approximate solution are not significant in a general description of the fluid. The solutions in Eqs. (3.10a) and (3.10b) provide only limited choice on the initial conditions, within the form as specified by the simple functions in these equations. However, a thin slab of matter with the right dimensions within the Landau model will likely capture the dominant features of the evolution dynamics.

It is useful to compare Landau hydrodynamics with Hwa-Bjorken hydrodynamics. We make the transformation $t = \tau\cosh y$, and $z = \tau\sinh y$. The energy density is then

$$\epsilon(\tau, y) = \epsilon_0 \exp\left\{-\tfrac{4}{3}\left[2\ln(\tau/\Delta) - \sqrt{[\ln(\tau/\Delta)]^2 - y^2}\right]\right\}. \quad (3.17)$$

In the region $y \ll \ln(\tau/\Delta)$, we have

$$\epsilon(\tau, y) \sim \epsilon_0 \exp\left\{-\tfrac{4}{3}\ln(\tau/\Delta)\right\} \propto \frac{1}{\tau^{4/3}}, \quad (3.18)$$

which is the Hwa-Bjorken hydrodynamics results. Therefore, in the region of small rapidities with $|y| \ll \ln(\tau/\Delta)$, Landau hydrodynamics and Hwa-Bjorken hydrodynamics coincide. In general, because Landau hydrodynamics covers a wider range of rapidities that may not be small, it is a more realistic description for the evolution of the hydrodynamical system.

IV. TRANSVERSE EXPANSION

The initial configuration is much thinner in the longitudinal direction than in the transverse directions. Therefore, in the first stage of the evolution during the fast one-dimensional longitudinal expansion, there is a simultaneous but slower transverse expansion. The difference in the expansion speeds allows Landau to treat the longitudinal and transverse dynamics as independent expansions. The rate of transverse expansion can then be obtained to provide an approximate description of the dynamics of the system.

We consider first the case of a central collision, for which $a_y = a_x = a$. The case of noncentral collisions is discussed in Sec. IX. The transverse expansion is governed by the Euler equation along one of the transverse directions, which can be taken to be along the x direction,

$$\frac{\partial T^{02}}{\partial t} + \frac{\partial T^{22}}{\partial x} = 0, \quad (4.1)$$

where

$$T^{02} = (\epsilon + p)u^0u^2 = \tfrac{4}{3}\epsilon u^0u^0v_x, \quad (4.2)$$

and we have used the relation $u^2 = u^0v_x$. The energy-momentum tensor T^{22} is

$$T^{22} = (\epsilon + p)u^2u^2 - pg^{22} = \tfrac{4}{3}\epsilon u^0u^0v_xv_x + p. \quad (4.3)$$

As the transverse expansion is relatively slow, we can neglect the first term on the right-hand side of the above expression and keep only the pressure term p.

In Landau's method of splitting the equations, one makes the approximation that during the first stage the quantities ϵ and y as a function of t and z have been independently determined in the one-dimensional longitudinal motion. Equation (4.1) can therefore be approximated as

$$\frac{4}{3}\epsilon u^0u^0\frac{\partial v_x}{\partial t} = -\frac{\partial p}{\partial x}. \quad (4.4)$$

The transverse displacement $x(t)$ (relative to zero displacement) as a function of time t is related to the acceleration $\partial v_z/\partial t$ by

$$x(t) = \frac{1}{2}\left(\frac{\partial v_x}{\partial t}\right)t^2. \quad (4.5)$$

The pressure is $p = \epsilon/3$ at the center of the transverse region and is zero at the radial surface $a/2$. Therefore the equation for the displacement is given from Eq. (4.4) by

$$\frac{4}{3}\epsilon u^0u^0\frac{2x(t)}{t^2} = \frac{\epsilon}{3a/2}. \quad (4.6)$$

We note that there is a factor of 4 arising from the ratio of $4\epsilon/3$ from $(\epsilon + p)$ on the left-hand side relative to $\epsilon/3$ from the pressure p on the right-hand side. However, in the original formulation of Landau [6,7], this factor of 4 is taken to be unity for an order of magnitude estimate of the transverse displacement. For our purpose of making quantitative comparison with experimental data, this factor of 4 cannot be neglected.

From Eq. (4.6), the transverse displacement $x(t)$ during the longitudinal expansion increases as

$$x(t) = \frac{t^2}{4au^0u^0} = \frac{t^2}{4a\cosh^2 y}. \quad (4.7)$$

V. SECOND STAGE OF CONIC FLIGHT

Landau suggested that when the transverse displacement $x(t)$ is equal to a at $t = t_{\rm FO}$, we need to switch to a new type of solution in the second stage of fluid dynamics. With the fluid element beyond the initial transverse dimension, hydrodynamical forces become so small that they can be neglected in the hydrodynamical equations at these locations and the flow rapidity y can be assumed to be frozen for $t \geqslant t_{\rm FO}$. This is equivalent to freezing the opening polar angle θ

between the fluid trajectory and the collision axis. The motion of the fluid element with a fixed polar angle can be described as a "three-dimensional" conic flight. In mathematical terms, Landau's condition for rapidity freeze-out occurs at $t_{\rm FO}(y)$, which satisfies [6,7]

$$x(t_{\rm FO}) = a. \tag{5.1}$$

As determined from Eqs. (4.7) and (5.1), rapidity freeze-out takes place at

$$t_{\rm FO}(y) = 2au^0 = 2a\cosh y. \tag{5.2}$$

The set of the $(t_{\rm FO}(y), y)$ points lie on the curve of the proper time, $\tau_{\rm FO} = 2a$. Thus, Landau's physical freeze-out condition, Eq. (5.1), corresponds to particle rapidities freezing-out at a fixed proper time,

$$\tau_{\rm FO} = 2a. \tag{5.3}$$

In a conic flight with an opening polar angle θ within an angle element $d\theta$, the energy-momentum tensor and the entropy flux within the cone element must be conserved as a function of time. The cross sectional area of such a cone element is $2\pi x dx$. So the conservation of energy and entropy conic flow correspond to

$$dE = \epsilon u^0 u^0 2\pi x dx = \text{constant}, \tag{5.4}$$

and

$$dS = \sigma u^0 2\pi x dx = \epsilon^{3/4} u^0 2\pi x dx = \text{constant}. \tag{5.5}$$

Dividing the first equation by the second equation, we get

$$\epsilon^{1/4} u^0 = \text{constant}, \tag{5.6}$$

which gives

$$\epsilon \propto \frac{1}{(u^0)^4}. \tag{5.7}$$

On the other hand, in the conic flight, x and dx are proportional to t. Hence, Eq. (5.4) gives

$$\epsilon u^0 u^0 t^2 = \text{constant}. \tag{5.8}$$

Eqs. (5.7) and (5.8) yield the dependence of various quantities as a function of t,

$$\epsilon \propto \frac{1}{t^4}, \quad \sigma \propto \frac{1}{t^3}, \quad \text{and} \quad u^0 \propto t. \tag{5.9}$$

These equations give the solution of the evolution of the fluid elements as a function of time in the second stage. By matching the solutions at $t = t_{\rm FO}(y)$, the energy density and velocity fields at the second stage for $t \geqslant t_{\rm FO}(y)$ are

$$\epsilon(t, y) = \epsilon(t_{\rm FO}, y) t_{\rm FO}^4 / t^4 \tag{5.10a}$$

$$u^0(t, y) = u^0(t_{\rm FO}, y) t / t_{\rm FO}. \tag{5.10b}$$

VI. RAPIDITY DISTRIBUTIONS IN HIGH-ENERGY HEAVY-ION COLLISIONS

The picture that emerges from Landau hydrodynamics can be summarized as follows. For an initial configuration of a thin disk of dense matter at a high temperature and pressure, the first stage of the motion is a one-dimensional longitudinal expansion with a simultaneous transverse expansion. The transverse expansion leads to a transverse displacement. When the magnitude of the transverse displacement exceeds the initial transverse dimension, forces acting on the fluid element become small and the fluid elements proceed to the second stage of conic flight with a frozen rapidity. As the transverse displacement depends on rapidity, and the transverse displacement magnitude decreases with increasing rapidity magnitude, the moment when the fluid element switches from the first stage to the second stage depends on the rapidity. The final rapidity distribution of particles is therefore given by the rapidity distribution of the particles at the matching time $t_{\rm FO}(y)$.

We first evaluate the entropy distribution as a function of rapidity y and time t in the first stage of hydrodynamics. Consider a slab element dz at z at a fixed time t. The entropy within the slab element is

$$dS = \sigma u^0 dz. \tag{6.1}$$

Using Eq. (3.11), we can express z as a function of t and rapidity y during the one-dimensional longitudinal expansion,

$$z = t\sinh y/\cosh y. \tag{6.2}$$

For a fixed value of t, we therefore obtain

$$dS = \sigma\, t\, dy/\cosh y. \tag{6.3}$$

The entropy density σ is related to ϵ by $\sigma = c\epsilon^{3/4}$ and ϵ is given by Eq. (3.10a). We obtain the rapidity distribution at the time t,

$$dS = c\epsilon_0^{3/4} \exp\{-(y_+ + y_- - \sqrt{y_+ y_-})\}\, t\, dy/\cosh y. \tag{6.4}$$

In the second stage, different fluid elements with different rapidities switch to conic flight at different time $t_{\rm FO}(y)$. The rapidity is frozen after $t > t_{\rm FO}(y)$. The final rapidity distribution after freeze-out needs to be evaluated at the switching time $t = t_{\rm FO}(y)$

$$dS = c\epsilon_0^{3/4} \left[\exp\{-(y_+ + y_- - \sqrt{y_+ y_-})\}\frac{t}{\cosh y}\right]_{t=t_{\rm FO}(y)} dy. \tag{6.5}$$

To evaluate the square-bracketed quantity at $t = t_{\rm FO}(y)$, we obtain from Eqs. (3.8) and (6.2) that

$$e^{y_\pm} = \frac{t}{\Delta}\frac{e^{\pm y}}{\cosh y}. \tag{6.6}$$

Therefore, we have

$$e^{y_\pm}|_{t=t_{\rm FO}(y)} = \frac{t_{\rm FO}(y)}{\Delta}\frac{e^{\pm y}}{\cosh y} = \frac{2a}{\Delta}e^{\pm y}, \tag{6.7}$$

which gives

$$y_\pm|_{t=t_{\rm FO}(y)} = \ln(2a/\Delta) \pm y. \tag{6.8}$$

We note that

$$\ln(2a/\Delta) = y_b = L + \ln 2, \tag{6.9}$$

where y_b is the beam rapidity in the center-of-mass system,

$$y_b = \cosh^{-1}(\sqrt{s_{NN}}/2m_p) \doteq \ln(\sqrt{s_{NN}}/m_p). \tag{6.10}$$

The rapidity distribution of Eq. (6.5) is therefore

$$dS = c\epsilon_0^{3/4} 2a \exp\left\{-2y_b + \sqrt{y_b^2 - y^2}\right\} dy. \quad (6.11)$$

As the entropy is proportional to the number of particles, we obtain the rapidity distribution

$$dN/dy \propto \exp\left\{\sqrt{y_b^2 - y^2}\right\}, \quad (6.12)$$

which differs from Landau's rapidity distribution of Eq. (1.3).

While many steps of the formulation are the same, the main difference between our formulation and Landau's appears to be the additional factor of 2 in Eqs. (6.7) and (5.2) in the new formulation. This factor can be traced back to the factor of 4 in the ratio of $4\epsilon/3$ from $(\epsilon + p)$ on the left-hand side of Eq. (4.6) and $\epsilon/3$ from the pressure p on the right-hand side. In Landau's formulation, this factor of 4 is taken to be unity for an order-of-magnitude estimate of the transverse expansion.

VII. COMPARISON OF LANDAU HYDRODYNAMICS WITH EXPERIMENTAL RAPIDITY DISTRIBUTIONS

Figure 3 gives the theoretical and experimental rapidity distributions for $\pi^+, \pi^-, K^+, K^-, p$, and $\bar{p}$ at $\sqrt{s_{NN}} = 200$ GeV [1]. The beam rapidity is $y_b = 5.36$, and the logarithm of the Lorentz contraction factor is $L = 4.67$. The solid curves give the modified distribution of Eq. (6.12), whereas the dashed curves are the Landau distribution of Eq. (1.3). The theoretical distributions for different types of particles have been obtained by keeping the functional forms of the distribution and fitting an overall normalization constant to the experimental data. We observe that Landau rapidity distributions are significantly narrower than the experimental rapidity distributions, whereas the modified distribution of Eq. (6.12) gives theoretical results that agree better with experimental data.

As a further comparison, we show theoretical distributions calculated with the Gaussian distribution of Eq. (1.1) as the dashed curves in Fig. 3. We find that except for the region of large rapidities, the Gaussian distribution is a good representation of the modified Landau distribution. The close similarity between the modified distribution (6.12) and the Gaussian distribution (1.1) explains the puzzle mentioned in the Introduction. The Gaussian distribution and the original Landau distribution are different distributions. Past successes of the Gaussian distribution in explaining experimental rapidity data [1–3] arise, not because it is an approximation of the original Landau distribution (1.3), but because it is in fact close to the modified Landau distribution (6.12) that derives its support from a careful reexamination of Landau hydrodynamics.

We compare theoretical distributions with the π^- rapidity distribution for collisions at various energies. The solid curves in Fig. 4 are the results from the modified distribution of Eq. (6.12) with the y_b parameter, whereas the dashed curves are the Landau distribution of Eq. (1.3) with the L parameter. The experimental data are from the compilation of Ref. [1]. The modified distributions of Eq. (6.12) give a better agreement with experimental data than the original Landau distributions.

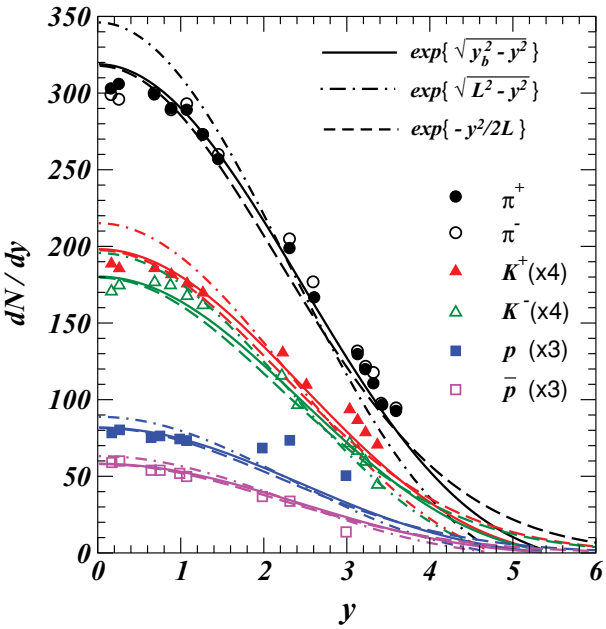

FIG. 3. (Color online) Comparison of experimental rapidity distribution with theoretical distribution in the form of $dN/dy \propto \exp\{\sqrt{y_b^2 - y^2}\}$ (solid curves), Landau's distribution $dN/dy(\text{Landau}) \propto \exp\{\sqrt{L^2 - y^2}\}$ (dashed-dot curves), and the Gaussian $dN/dy(\text{Gaussian}) \propto \exp\{-y^2/2L\}$ (dashed curves) for produced particles with different masses. Data are from Ref. [1] for AuAu collisions at $\sqrt{s_{NN}} = 200$ GeV.

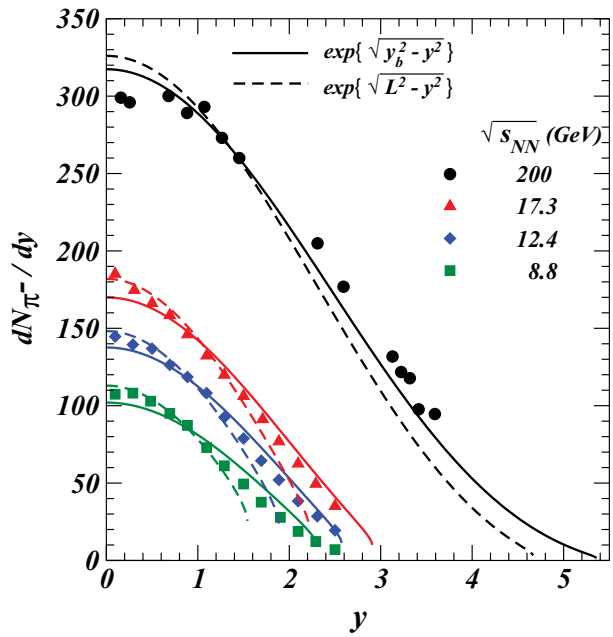

FIG. 4. (Color online) Comparison of experimental rapidity distribution with theoretical distribution in the form of $dN/dy \propto \exp\{\sqrt{y_b^2 - y^2}\}$ (solid curves) and Landau's distribution $dN/dy(\text{Landau}) \propto \exp\{\sqrt{L^2 - y^2}\}$ (dashed curves) for produced particles at different energies. Experimental dN_{π^-}/dy data are from the compilations in Ref. [1].

VIII. PREDICTIONS OF RAPIDITY DISTRIBUTIONS FOR LHC ENERGIES

We can rewrite the rapidity distribution of charged particles in terms of the normalized distribution dF/dy,

$$(dN_{\rm ch}/dy)/(N_{\rm part}/2) = [N_{\rm ch}/(N_{\rm part}/2)]dF/dy. \quad (8.1)$$

The normalized distribution dF/dy is

$$\frac{dF}{dy} = \begin{cases} A_{\rm norm}\exp\left\{\sqrt{y_b^2 - y^2}\right\} & \text{for modified distribution,} \\ A_{\rm norm}\exp\{\sqrt{L^2 - y^2}\} & \text{for Landau distribution,} \\ \frac{1}{\sqrt{2\pi L}}\exp\{-y^2/2L\} & \text{for Gaussian distribution,} \end{cases} \quad (8.2)$$

where $A_{\rm norm}$ is a normalization constant such that

$$\int dF/dy = 1. \quad (8.3)$$

With the knowledge of the total charged multiplicity from Fig. 1, and the shape of the rapidity distribution from Eq. (8.2), we can calculate $dN_{\rm ch}/dy/(N_{\rm part}/2)$ as a function of rapidity. Figure 5 gives the predicted rapidity distributions at LHC energies. For heavy-ion collisions at $\sqrt{s_{NN}} = 5.5$ TeV with full stopping, the maximum value of dN/dy per participant pair is about 22 at midrapidity. For pp collisions at $\sqrt{s_{NN}} = 14$ TeV with $\xi = 0.5$, the maximum dN/dy is approximately 24 at $y = 0$. The widths of the rapidity distributions are $\sigma_y \sim 3$. The solid curves are for the modified distribution, the dashed-dot curves are for the original Landau distribution, and the dashed curves are for the Gaussian distribution.

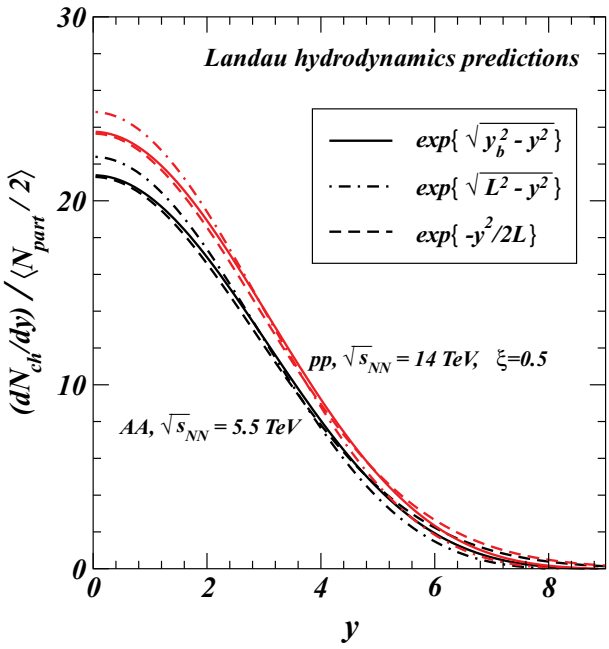

FIG. 5. (Color online) The predicted rapidity distributions $dN_{\rm ch}/dy/(N_{\rm part}/2)$ of charged particles produced in pp collisions at $\sqrt{s_{NN}} = 14$ TeV with $\xi = 0.5$, and AA collisions at $\sqrt{s_{NN}} = 5.5$ TeV with full stopping in Landau hydrodynamics. The solid curves are obtained with the modified distribution, the dashed-dot curves are obtained with the original Landau distribution, and the dashed curves with the Gaussian distribution.

IX. GENERALIZATION TO NONCENTRAL COLLISIONS

In noncentral collisions, the transverse radius $a_\phi/2$ will depend on the azimuthal angle ϕ measured relative to the x axis as depicted in Fig. 2. Following the same Landau arguments as in the central collision case, Eq. (4.6) for the transverse displacement can be generalized to be

$$\frac{4}{3}\epsilon u^0 u^0 \frac{2\rho(\phi,t)}{t^2} = \frac{\epsilon}{3a_\phi/2}, \quad (9.1)$$

where $\rho(\phi, t)$ is the transverse displacement at azimuthal angle ϕ. The transverse displacement depends on ϕ and t as

$$\rho(\phi,t) = \frac{t^2}{4a_\phi u^0 u^0} = \frac{t^2}{4a_\phi \cosh^2 y}. \quad (9.2)$$

The Landau condition for the onset of the second stage is the condition that the transverse displacement $\rho(\phi, t)$ is equal to the transverse dimension a_ϕ,

$$\rho(\phi, t_{\rm FO}) = a_\phi. \quad (9.3)$$

Thus, in the case of noncentral collision, the Landau condition of Eq. (5.1) is changed to

$$t_{\rm FO}(y,\phi) = (a_\phi/a) \times 2a\cosh y. \quad (9.4)$$

Following the same argument as before, Eq. (6.8) for the noncentral collision case becomes

$$y_\pm|_{t=t_{\rm FO}(y,\phi)} = \ln(a_\phi/a) + \ln(2a/\Delta_b) \pm y, \quad (9.5)$$

where the longitudinal thickness of the initial slab Δ_b depends on the impact parameter b. As a consequence, the rapidity distribution for this noncentral collision is

$$\frac{dN}{dy} \propto \exp\left\{\sqrt{\ln(2a/\Delta_b) + \ln(a_\phi/a)]^2 - y^2}\right\}. \quad (9.6)$$

X. CORRECTIONS TO THE LANDAU MODEL

Results in the last few sections deal with the Landau model in its traditional form. It is gratifying that gross features of many measured quantities are reproduced well. The Landau model with the modified distribution (6.12) can be considered a good first approximation. Corrections and refinements are expected to be small and need to be included as physical considerations and experimental data demand. In this respect, it is useful to examine two important corrections arising from uncertainties in the initial configuration and the final freeze-out condition.

The Landau model assumes that the initial configuration corresponds to a disk of thickness $\Delta =$ (nuclear diameter a)$/\gamma$ as given by Eq. (3.1). Landau's hydrodynamical expansion commences at the end of the initial compression, with the formation of shock waves already at hand. However, the thickness of the initial compressed shock waves arises from balancing energy and momentum following the Rankine-Hugoniot boundary conditions across the shock

front [24,26]. The longitudinal thickness of the compressed region (shock region) depends not only on the diameter a of the nuclei but also on the equation of state and the collision energies. Thus, although the initial nuclear diameter a is an important scaling parameter as used by Landau, the longitudinal thickness of the compressed region may deviate from the Landau's estimate of a/γ because of the equation of state and collision energy considerations. The equation of state at AGS energies is more dominated by baryons while the equation of state from RHIC collisions will be dominated by gluons and quarks. How the effects of the speed of sound can affect the rapidity distribution in the Landau model have been examined recently by Bialas and his collaborators [19] and by Mohanty and Alam [16]. There is furthermore the possibility of a much more extended longitudinal configuration in the initial stages of highly relativistic collisions in the string rope description of the initial longitudinal compression [27]. In that description, the extension will depend on the string tension of the rope between the separating partons, as investigated by Magas and his collaborators [27]. The observed strong azimuthal anisotropy as represented by the azimuthal Fourier b_n coefficients of Ref. [28] (or the v_n coefficients in the later notation of Ref. [29] for elliptic flow [30,31]) may indicate this extended initial state of Ref. [27] and an initial longitudinal dimension greater than Landau's estimate.

There is another important correction to Landau's initial longitudinal thickness because of the spherical geometry of the nuclei. The Landau model assumes a initial longitudinal thickness of a/γ with a nearly uniform longitudinal distribution for a nucleus with a diameter of a in its own rest frame. However, the longitudinal distribution of a spherical nucleus is far from being uniform. A longitudinally uniform cylinder of the same volume in a transverse disk of diameter a will have a longitudinal thickness equal to $2a/3$, which is substantially smaller than the value of a assumed by Landau. The density distribution of a spherical nucleus is also not uniform in the transverse direction, when it is projected transversely.

All these corrections due to shock wave compression and spherical geometry are expected to scale with the nuclear diameter a. We can introduce phenomenologically a correction factor C_{init} to represent the effects of these scaled corrections so that the longitudinal thickness changes from $\Delta = a/\gamma$ to Δ',

$$\Delta \to \Delta' = C_{\text{init}} \times a/\gamma. \tag{10.1}$$

Upon replacing Δ by Δ', we get from Eqs. (6.9) and (6.12) that dN/dy is modified to become

$$\frac{dN}{dy} \propto \exp\{\sqrt{(y_b - \ln C_{\text{init}})^2 - y^2}\}. \tag{10.2}$$

Thus the thickness correction factor C_{init} leads to a logarithmic correction to the parameter y_b in Landau's distribution of Eq. (6.12). For example, the geometrical correction of $C_{\text{init}}(\text{geometrical}) \sim 2/3$ contribute to a positive value of $(-\ln C_{\text{init}}) \sim 0.405$, and a more extended initial shock wave region as in Ref. [27] will lead to a negative contribution to $(-\ln C_{\text{init}})$ and a narrower rapidity width. There is thus an interplay between the static geometrical effects and the dynamical effects due to compression and string rope extension.

There is an additional complication arising to the approximate freeze-out condition. Landau's freeze-out condition of $\tau_{\text{FO}} = 2a$ comes from his argument on the magnitude of the transverse displacement. Landau's freeze-out surface is a space-like surface with a normal pointing in the time-like direction. Important contributions on the freeze-out condition come from Cooper and Frye [12] who used a fixed temperature freeze-out condition. They found that the freeze-out surface in this case contains both the space-like portion and the time-like portion [12]. Another important contribution comes from Csernai [26] who used the Rankine-Hugoniot conditions to describe the freeze-out boundary. In this case the balance of the transport across the freeze-out surface leads to a modification of the transport equation for freeze-out [32]. In the unified description of Hwa-Bjorken and Landau hydrodynamics, Bialas and his collaborators [19] examined various freeze-out conditions for fixed t, τ, and temperature T and compared them with the original Hwa-Bjorken and Landau results. Using a new family of simple analytical hydrodynamical solutions, Csörgö and his collaborators [20] used the fixed temperature condition for the freeze-out. The effects of the speeds of sound and the freeze-out temperature on the rapidity distribution in the Landau model have been investigated recently by Beuf and his collaborators [21].

While there are many possible freeze-out conditions, the successes of Landau hydrodynamics suggest that Landau's freeze-out condition can be a crude first approximation and the correction is likely to be small and scale with the Landau freeze-out proper time $\tau_{\text{FO}} \sim 2a$. Phenomenologically it is therefore useful to introduce a corrective freeze-out factor C_{FO} to replacing τ_{FO} by τ'_{FO},

$$\tau_{\text{FO}} \to \tau'_{\text{FO}} = C_{\text{FO}} \times 2a. \tag{10.3}$$

From Eq. (6.9), this modification of the freeze-out proper time leads to a modification of the rapidity distribution from dN/dy of Eq. (6.12) that becomes

$$\frac{dN}{dy} \propto \exp\{\sqrt{(y_b + \ln C_{\text{FO}})^2 - y^2}\}. \tag{10.4}$$

Again, the correction factor C_{FO} leads to a logarithmic correction to y_b.

The measured rapidity distribution depends on the combination of both effects. Upon combining the initial condition and the freeze-out condition corrections from Eqs. (10.2) and (10.4), we obtain

$$\frac{dN}{dy} \propto \exp\{\sqrt{(y_b + \zeta)^2 - y^2}\}, \tag{10.5}$$

where the correction parameter ζ is

$$\zeta = -\ln C_{\text{init}} + \ln C_{\text{FO}}. \tag{10.6}$$

Our theoretical knowledge has not advanced to such an extent that we can separate out the different effects due to the initial conditions and the effects due to the freeze-out conditions as they closely interplay to give rise to the observed rapidity distribution. What is possible is to extract the deviations of the experimental data from the Landau model so that the small deviations may reveal useful information in future investigations. The agreement with experimental dN/dy data

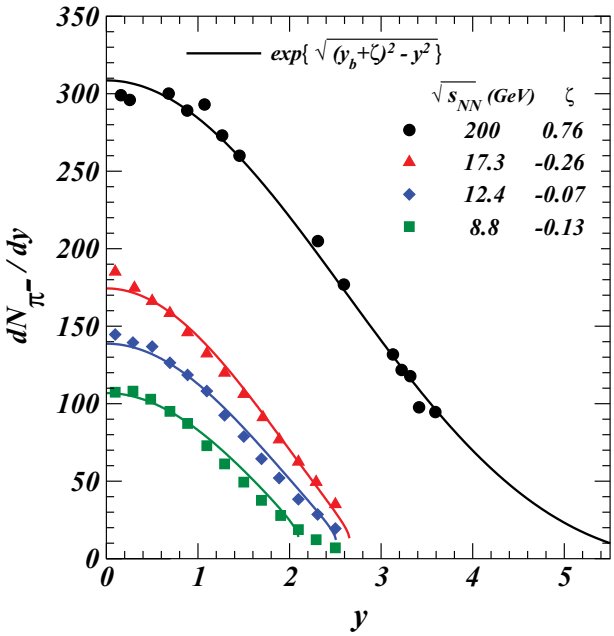

FIG. 6. (Color online) Comparison of experimental rapidity distributions with theoretical rapidity distributions dN_{π^-}/dy (solid curves), calculated with Eq. (10.5) at various energies. Experimental data points are from Ref. [1].

with theoretical predictions will be slightly improved when we include this correction parameter ζ. In Fig. 6, we use the experimental dN_{π^-}/dy data [1] and the distribution of Eq. (10.5) to extract the quantity ζ as a function of $\sqrt{s}$ shown in Table I. As a comparison, the corresponding values of y_b are also listed. One finds that for AGS and SPS energies, the combined effects of initial and freeze-out corrections lead to a small correction parameter ζ ranging from -0.07 to -0.26. The correction ζ is larger for RHIC energies and assumes the value of 0.76. In all cases, the magnitude of the correction parameter, $|\zeta|$, is much smaller than y_b, indicating the validity of the Landau model as a good first approximation. How the small correction ζ varies with collision energy is an interesting topic worthy of future investigations.

The particle multiplicity in the Landau model is also affected by the initial compressed volume and the bag constant as the observed particles are hadrons subject to the bag pressure of confined quarks and gluons [13]. The effect of the bag constant is, however, small for high-energy collisions [13].

TABLE I. The correction parameter ζ as a function of collision energy $\sqrt{s_{NN}}$.

$\sqrt{s_{NN}}$ (GeV)	ζ	y_b
200	0.76	5.362
17.3	−0.26	2.917
12.4	−0.07	2.575
8.8	−0.13	2.226

XI. CONCLUSIONS AND DISCUSSIONS

In many problems in high-energy collisions, such as in the description of the interaction of the jet or quarkonium with the produced dense matter, it is desirable to have a realistic but simple description of the evolution of the produced medium. Landau hydrodynamics furnishes such a tool for this purpose.

Recent successes of Landau hydrodynamics in explaining the rapidity distribution, total charged multiplicities, and limiting fragmentation [1–3] indicate that it contains promising degrees of freedom. Questions are, however, raised concerning the use of pseudorapidity or rapidity variables, the Gaussian form or the square-root exponential form of the rapidity distribution, and the values of the parameters in the rapidity distribution.

We start with the rapidity variable from the outset so that we do not need to worry about the question of the rapidity or the pseudorapidity variable. We follow the formulation of the Landau hydrodynamics by keeping careful track of the numerical constants that enter into the derivation. We confirm Landau's central results except that the approximate rapidity distribution obtained by Landau needs to be modified, when all numerical factors are carefully tracked. In particular, the rapidity distribution in the center-of-mass system should be more appropriately given as $dN/dy \propto \exp\{\sqrt{y_b^2 - y^2}\}$, where y_b is the beam nucleon rapidity, instead of the Landau original result of $dN/dy(\text{Landau}) \propto \exp\{\sqrt{L^2 - y^2}\}$. The modified distribution leads to a better description of the experimental data and thereby supports the approximate validity of Landau hydrodynamics as a description of the evolution of the produced bulk matter.

The modified distribution differs only slightly from the Gaussian distribution $dN/dy(\text{Gaussian}) \propto \exp\{-y^2/2L\}$, which has been used successfully and extensively in the literature [1–3,11]. This explains the puzzle we mention in the Introduction. Even though the Gaussian Landau distribution (1.1) is conceived as an approximate representation of the original Landau distribution (1.3) for the region of small rapidity with $|y| \ll L$, it differs from the original Landau distribution in other rapidity regions. The Gaussian distribution has been successfully used to explain experimental rapidity distribution data [1–3], not because it is an approximation of the original Landau distribution (1.3), but because it is in fact a good representation of the modified Landau distribution (6.12) that derives its support from a careful reexamination of Landau hydrodynamics. Thus, there is now a firmer theoretical support for the Gaussian distribution (1.1) owing to its similarity to the modified distribution of Eq. (6.12).

The need to modify Landau's original distribution should not come as a surprise, as the original Landau distribution was intended to be qualitative. Our desire to apply it quantitatively therefore led to a more stringent reexamination, with the result of the modification as we suggest. The quantitative successes of the modified distribution in Landau hydrodynamics make it a useful tool for many problems in high-energy heavy-ion collisions.

Despite these successes, many problems will need to be examined to make the Landau model an even better tool. We have discussed the important effects of the initial configuration

and the final freeze-out condition in Sec. X. They lead to uncertainties that give rise to a logarithmic correction parameter ζ with a magnitude much smaller than y_b. How the small correction ζ varies with the collision energy is a subject worthy of further investigations. We can also outline a few others that will need our attention. The distribution so far deals with flow rapidity of the fluid elements, and the thermal distribution of the particles inside the fluid element has not been included. The folding of the thermal distribution of the particles will broaden the rapidity distribution and should be the subject of future investigations. Another improvement is to work with a curvilinear coordinate system in the transverse direction to obtain the transverse displacement. This will improve the description of the matching time in the transverse direction. One may wish to explore other forms of the freeze-out condition instead of Landau's transverse displacement condition to see how sensitively the results can depend on the freeze-out condition. Finally, as the approximate solution for the one-dimensional longitudinal expansion is also available, it may also be of interest to see how much improvement there can be in obtaining the matching time estimates that enter into the rapidity freeze-out condition.

ACKNOWLEDGMENTS

The author thanks Professor D. Blaschke for his hospitality at the the Helmholtz International Summer School, July 12–26, 2008, Bogoliubov Laboratory of Theoretical Physics, Dubna, Russia, where this work on Landau hydrodynamics was initiated as lecture notes. This research was supported in part by the Division of Nuclear Physics, U.S. Department of Energy, under Contract DE-AC05-00OR22725, managed by UT-Battelle, LLC.

[1] M. Murray (Brahms Collaboration), J. Phys. G **30**, S667 (2004); I. G. Bearden *et al*. (BRAHMS Collaboration), Phys. Rev. Lett. **94**, 162301 (2005); M. Murray (Brahms Collaboration), J. Phys. G **35**, 044015 (2008).
[2] P. Steinberg, Nucl. Phys. **A752**, 423 (2005).
[3] P. Steinberg, in Proceedings of 3rd International Workshop on Critical Point and Onset of Deconfinement, Florence, Italy, 3–6 July, 2006, arXiv:nucl-ex/0702019.
[4] R. C. Hwa, Phys. Rev. D **10**, 2260 (1974).
[5] J. D. Bjorken, Phys. Rev. D **27**, 140 (1983).
[6] L. D. Landau, Izv. Akad. Nauk SSSR **17**, 51 (1953).
[7] S. Z. Belenkij and L. D. Landau, Usp. Fiz. Nauk **56**, 309 (1955); Nuovo Cimento Suppl. **3**, 15 (1956).
[8] I. M. Khalatnikov, Zh. Eksp. Teor. Fiz. **27**, 529 (1954).
[9] S. Z. Belenkij and G. A. Milekhin, Zh. Eksp. Teor. Fiz. **29**, 20 (1956) [Sov. Phys. JETP **2**, 14 (1956)]; I. L. Rosental, Zh. Eksp. Teor. Fiz. **31**, 278 (1957) [Sov. Phys. JETP **4**, 217 (1959)]; G. A. Milekhin, Zh. Eksp. Teor. Fiz. **35**, 978 (1958) [Sov. Phys. JETP **8**, 682 (1959)]; G. A. Milekhin, Zh. Eksp. Teor. Fiz. **35**, 1185 (1958) [Sov. Phys. JETP **8**, 829 (1959)].
[10] S. Amai, H. Fukuda, C. Iso, and M. Sato, Prog. Theor. Phys. **17**, 241 (1957).
[11] P. Carruthers and Minh Doung-van, Phys. Rev. D **8**, 859 (1973).
[12] F. Cooper and G. Frye, Phys. Rev. D **10**, 186 (1974).
[13] F. Cooper, G. Frye, and E. Schonberg, Phys. Rev. D **11**, 192 (1975).
[14] S. Chadha, C. S. Lam, and Y. C. Leung, Phys. Rev. D **10**, 2817 (1974).
[15] D. K. Srivastava, J. Alam, and B. Sinha, Phys. Lett. **B296**, 11 (1992); D. K. Srivastava, J. Alam, S. Chakrabarty, B. Sinha, and S. Raha, Ann. Phys. **228**, 104 (1993); D. K. Srivastava, J. Alam, S. Chakrabarty, S. Raha, and B. Sinha, Phys. Lett. **B278**, 225 (1992).
[16] B. Mohanty and J. Alam, Phys. Rev. C **68**, 064903 (2003).
[17] Y. Hama, T. Kodama, and O. Socolowski, Jr., Braz. J. Phys. **35**, 24 (2005); C. E. Aguiar, T. Kodama, T. Osada, and Y. Hama, J. Phys. G **27**, 75 (2001).
[18] S. Pratt, Phys. Rev. C **75**, 024907 (2007).
[19] A. Bialas, R. A. Janik, and R. Peschanski, Phys. Rev. C **76**, 054901 (2007).
[20] T. Csörgö, M. I. Nagy, and M. Csanád, Phys. Lett. **B663**, 306 (2008).
[21] G. Beuf, R. Peschanski, and E. N. Saridakis, arXiv:0808.1073.
[22] E. K. G. Sarkisyan and A. S. Sakharov, AIP Conf. Proc. **828**, 35 (2006); E. K. G. Sarkisyan and A. S. Sakharov, arXiv:hep-ph/0410324.
[23] C. Y. Wong, *Introduction to High-Energy Heavy-Ion Collisions* (World Scientific, Singapore, 1994).
[24] C. Y. Wong and T. A. Welton, Phys. Lett. **B49**, 243 (1974).
[25] M. Basile *et al*., Nuovo Cimento A **65**, 400 (1981); M. Basile, Nuovo Cimento A **67**, 244 (1981).
[26] L. P. Csernai, Sov. Phys. JETP **65**, 216 (1987).
[27] V. K. Magas, L. P. Csernai, and D. D. Strottman, Phys. Rev. C **64**, 014901 (2001); V. K. Magas, L. P. Csernai, and D. D. Strottman, Nucl. Phys. **A712**, 167 (2002).
[28] C. Y. Wong, Phys. Lett. **B88**, 39 (1978).
[29] S. Voloshin and Y. Zhang, Z. Phys. C **70**, 665 (1996).
[30] P. Danielewicz and G. Odyniec, Phys. Lett. **B157**, 146 (1985).
[31] J. Y. Ollitrault, Phys. Rev. D **46**, 229 (1992).
[32] V. K. Magas, L. P. Csernai, E. Molnar, A. Nyiri, and K. Tamosiunas, Eur. Phys. J. A **25**, 65 (2005).